International Journal for Housing Science and Its Applications
Publish August 4, 2025. Volume 46, Issue 3 Pages 3351-3359

https://doi.org/10.70517/ijhsa463283

Innovative Application of High-Precision Three-dimensional Modeling in Cultural Heritage Protection--The Case of Tomb Room Mural Painting

Sukai Liu[1,*]
[1] College of Art and Design, Pingdingshan University, Pingdingshan, Henan, 467000, China
Corresponding authors: (e-mail: lsk20246688@163.com).

Abstract Intangible cultural heritage is the precipitation of civilization in the process of human development and the inheritance of people's generational spirit. The study focuses on the application of 3D modeling technology in cultural genetic protection, innovatively proposes a 3D point cloud edge extraction algorithm based on Gaussian mapping clustering, using K-nearest neighbor search, Gaussian mapping and K-means clustering algorithms to realize the extraction of edge features of the mural paintings of the tombs, in order to assist the restoration of the mural paintings and the protection of inheritance. Through the experiments on the public dataset and the tomb chamber mural dataset, it is found that the results of this paper's method are better than the comparison method in all three indexes, and the ODS, OIS and AP values of this paper's method are improved by 2.19%, 0.95% and 1.78% in the public dataset, and 3.35%, 4.05% and 5.24% in the tomb chamber mural dataset, respectively. In addition, the edge extraction results on the sample of tomb chamber murals also confirm the effectiveness and efficiency of the method. The results show that the proposed method has a positive effect on the digital preservation and subsequent restoration of cultural heritage.

Index Terms three-dimensional modeling, K-nearest neighbor search, Gaussian mapping, edge extraction, cultural heritage preservation

I. Introduction

Cultural heritage, including tangible cultural heritage such as historical buildings, archaeological sites, artifacts and handicrafts, and intangible cultural heritage such as languages, traditions, beliefs and rituals, is a bridge between the past and the present [1], [2]. It not only carries the memory of human history, but also symbolizes cultural diversity and national identity [3]. Taking tomb murals as an example, the scenes depicted in them contain a true portrayal of human life, and they also epitomize the image of the ancient society, which can strongly corroborate the historical development and changes of the Chinese society as well as culture in historical archaeological research [4]-[6]. However, although the value of tomb murals is high, it is difficult to present and protect this precious cultural heritage with the existing technology [7]. Traditional conservation methods, such as physical restoration, on-site conservation and relocation conservation, can slow down the rate of destruction of tomb chamber murals to a certain extent, but they often have limitations [8]-[10]. Physical restoration may cause secondary damage to the original materials, and on-site conservation is difficult to cope with large-scale natural disasters [11], [12]. Relocation conservation, on the other hand, may change the original environment and context of the tomb murals, affecting the integrity of their historical and cultural values [13], [14]. In addition, the cost of traditional conservation methods is often very high, requiring a large amount of human, material and financial investment, which is an unbearable burden for the tomb chamber mural painting conservation projects [15], [16].

With the progress of scientific and technological society, computer technology has been popularized, and three-dimensional modeling technology has been widely used in the field of cultural heritage protection. Digital reconstruction of cultural heritage through high-precision 3D scanning and modeling creates accurate virtual copies, and even if the original cultural heritage is damaged, its digital copy can retain its historical and cultural value [17]-[19]. In addition, the highly interactive and immersive atmosphere of 3D virtual space provides a new way to display and educate cultural heritage, allowing users to interact with the murals in the virtual environment and gain a deeper understanding of the history and culture behind them [20]-[22]. Based on this, high-precision 3D modeling technology contributes to the protection and inheritance of global cultural heritage, effectively overcomes the limitations of traditional protection methods, and opens up new paths for the protection and inheritance of cultural heritage [23], [24].

The study discusses the application of 3D modeling in cultural heritage protection from three aspects: opening up communication channels, restoring the details of cultural relics and optimizing the management mode. Taking the digital protection of tomb chamber murals as an example, a K-mean method based on Gaussian mapping is proposed, in which the K-nearest-neighbor search of the target points is performed first, and then Gaussian mapping is performed on the unit normal vectors of the set of triangles consisting of the target points and their nearest-neighbor points. The contour coefficient is selected as the clustering validity index, and the optimal number of clusters is determined, and the feature lines of the 3D laser point cloud model are obtained according to the law of the clustering distribution of different surfaces. The BSDS500 dataset and the tomb mural dataset are selected as the experimental objects, and ODS, OIS and AP are used as the evaluation indexes to carry out the comparison experiments of the algorithms. Then, the edge extraction experiments are carried out on different point cloud objects, and compared and analyzed in terms of edge extraction effect and extraction time, respectively, to explore the application effect of the proposed 3D point cloud edge extraction algorithm.

II. Application of 3D modeling in cultural heritage preservation

In the process of cultural heritage protection, how to accurately and quickly acquire digital surface models of cultural relics turns out to be an important issue because cultural relics are characterized by diverse shapes and textures and are not easily accessible. Considering that most of the cultural relics are not directly accessible and the non-destructive testing of cultural relics requires high accuracy, non-contact 3D information acquisition technologies such as 3D laser scanning technology, unmanned aerial vehicle, and close-up photogrammetry have been applied to the protection of cultural relics. The application scenarios of 3D modeling technology in cultural heritage protection are mainly divided into the following aspects.

II. A. Opening up communication channels

Firstly, the digital 3D modeling technology has opened up a new carrier way for the preservation and dissemination of intangible cultural heritage. Three-dimensional digital modeling data collection and the application of 3D digital modeling technology provide new ways and platforms for the preservation and dissemination of intangible cultural heritage. Through 3D digital modeling technology, intangible cultural heritage can be presented to the public in a more intuitive and vivid way, thus promoting its inheritance and exchange. Tools such as digital archiving, virtual exhibitions and online platforms provide a wider range of spaces and channels for the safeguarding and dissemination of ICH.

II. B. Cultural heritage restoration

Secondly, the three-dimensional digital twin model realizes the cross-border innovative transformation and sharing of the “authenticity” of intangible cultural heritage. Three-dimensional digital twin modeling can improve the precision and realism of digital twins, and digital twin data collection of intangible cultural heritage can accurately restore the subtle features of intangible cultural heritage in order to maintain its uniqueness and authenticity. While realistically reproducing the traditional features of ICH, the 3D digital modeling technology can also establish digital archives and build online platforms so that people from different regions and cultural backgrounds can share experiences, resources and exchange practices more easily through the digital platforms, thus promoting the safeguarding and transmission of ICH. Cross-border cooperation and sharing provide broader space and possibilities for the safeguarding of intangible cultural heritage.

II. C. Optimization of management models

Thirdly, digital technology has changed the management and governance mode of intangible cultural heritage. Through three-dimensional digital modeling of ICH, the online platform built by the Internet and social media can be used to firstly promote the democratization of public participation in the safeguarding of ICH, so that more people can be involved in the process of safeguarding ICH, and people's sense of social responsibility and participation can be enhanced. Social participation and democratization are important safeguards and driving forces for ICH safeguarding. Secondly, the digital archive management of intangible cultural heritage improves the management efficiency and protection level, and enhances the protection level of intangible cultural heritage.

III. 3. Gaussian mapping clustering based point cloud edge extraction method

As a carrier of history and culture, tomb murals carry the rise and fall of human civilization. Accurate and clear extraction of the contour lines of tomb murals is crucial for the digital conservation and subsequent restoration of murals. Based on this, this paper applies high-precision 3D modeling technology to the protection of tomb murals, explores the edge extraction technology of tomb murals, and proposes a point cloud edge extraction method based on Gaussian mapping clustering.

III. A. Algorithm overview

The flow of the proposed edge extraction algorithm is shown in Fig. 1, for the extraction of feature lines firstly, K nearest neighbor search is used to find the k proximity points of each target point of the point cloud data, and then the target point and any two of its neighboring points are arranged and combined to form a triangle, and its unit normal vector is derived, and then it is Gaussian mapped, and finally clustering method is utilized to achieve the purpose of the feature point discriminations.

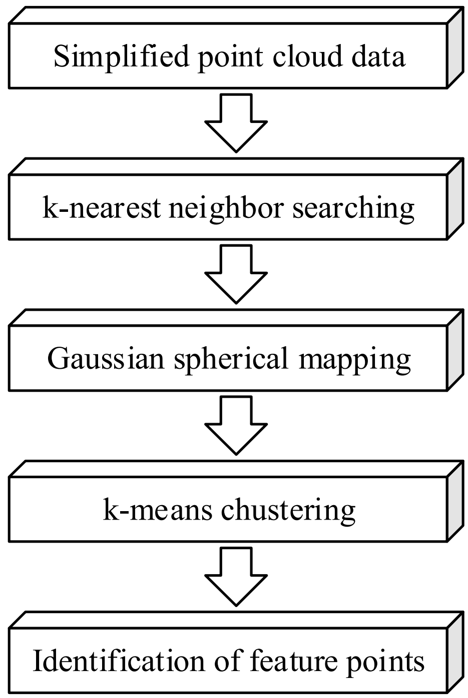

Figure 1: Process of edge extraction algorithm

III. B. Point cloud edge extraction method

III. B. 1) K Nearest Neighbor Algorithm

K Nearest Neighbor (KNN) classification algorithm, is a more mature classification algorithm, is also one of the most classic methods in machine learning algorithms, the basic idea is: first calculate the distance or similarity between the samples to be classified and the known classification category samples, to find in the feature space k the most similar (i.e., the closest to the samples to be classified in the feature space with the closest k close neighbors) of the nearest neighbor relationship points. Secondly, the selected k nearest neighbors are all correctly classified, and the attributes of the samples to be classified are judged according to the categories to which these samples belong, this step in the decision to decide on the attributes of the category is based only on the category of the nearest neighbors of one or more samples to be classified, and if the samples to be classified by the k nearest neighbors all belong to the same category, the samples to be classified belong to the category as well. Otherwise, each candidate category will be judged and the category of the sample to be classified will be finalized according to certain rules. The K nearest neighbor algorithm measures the weights of the other categories of samples around the point to be tested according to its location, so as to categorize the point to be tested into a class where the number of samples of the other categories is higher or the weights are larger, and such categorization decision rules follow majority voting.

The selection of the k value, the distance measure and the classification decision rule in the KNN algorithm are the three basic elements of the algorithm.

(1) Selection of k values. The selection of k values has a crucial role in the classification results of the KNN algorithm. k value if small, the classification results are similar to only a few training sample categories that are closer to the point to be measured. If the value of k is large, it leads to the fact that the training samples that are far away from the point to be tested will also play a role in the classification results of the point to be tested, which is prone to error. Cross-validation is usually used to select the optimal k value, and the k value is usually small.

(2) Distance metric. The distance metric in the KNN algorithm generally uses Euclidean distance.

(3) Classification decision rule: Most of the classification decision rules in the KNN algorithm follow the majority voting rule, i.e., when the exemption value is selected, the classification of the point to be measured is based on the class of the point to be measured decided by the majority class of the k nearest training samples.

The step-by-step process of the KNN algorithm is as follows:

Step 1, collect raw data and construct the training sample set.

Step 2, an initial value of the k value is set and the raw data is preprocessed for calculating the distance metric and the data is preferably structured.

Step 3, compute the distance metric. Assume that the samples belong to the n-dimensional space R^n, and the samples $x_i = (x_{i1}, x_{i2}, \ldots, x_{im}) \in R^n$, where x_{im} denotes the m-feature dimension of the i th sample. The distance metric is computed as follows.

The Minkowski distance between two sample points x_i and y_i in n-dimensional space is defined as:

$$d = \left(\sum_{i=1}^{n} | x_i - y_i |^p \right)^{\frac{1}{p}} \tag{1}$$

Minkowski distance is the definition of a class of distances, should be for the different values of p in the formula, you can get the Euclidean distance, Manhattan distance and Chebyshev distance, etc., in the KNN algorithm, the most commonly used Euclidean distance $p = 2$, the formula is:

$$d = \left(\sum_{i=1}^{n} | x_i - y_i |^2 \right)^{\frac{1}{2}} = ((x-y)^T (x-y))^{\frac{1}{2}} = \| x - y \|_2 \tag{2}$$

Step 4, for the input point to be measured, which is surrounded by $x_1, x_2, ..., x_k$ totaling k closest sample points, given a classification task, the classification function is:

$$f : x \to \{c_1, c_2, ..., c_i\} \tag{3}$$

where c_i is the category labeling and x is the sample of points to be measured. Construct the discriminant function $g_k(x)$, defined as follows:

$$g_k(x) = \begin{cases} 1, f(x) = c_i \\ 0, f(x) \neq c_i \end{cases} \tag{4}$$

where c_i is the true category labeling of x and k denotes the number of nearest neighbors using the KNN algorithm.

The objective function that defines the correct classification of the nearest neighbors of a particular sample is:

$$F(x) = arm \max \sum_{i=1}^{k} g_k(x) \tag{5}$$

In step 5, a classification operation is performed on the sample to be tested using the majority voting mechanism as a basic criterion.

III. B. 2) Gaussian Mapping

Currently, Gaussian mapping has been applied to the neighborhoods of point cloud fitting, surface identification, and point cloud classification. Gaussian mapping is defined as follows: for any segmented smooth spatial three-dimensional surface, first compute the unit normal vectors of all the points of the point cloud on the surface, and move the starting point of the obtained normal vectors to the center of the predefined unit sphere, and the end point of the normal vectors falls directly on the surface of the unit sphere, and the projection formed by projecting the set of projected points is called the Gauss map of the surface. The process of mapping the normal vectors of the points on the surface onto the sphere of the unit ball is called Gauss mapping, and the unit ball is called the Gauss sphere. For classifying a complete three-dimensional model, whose surface is usually composed of many surfaces, the set of Gaussian maps of individual surfaces that have been Gaussian mapped is called the Gaussian map of the model.

All points on a plane are planar points, and all points on a cylindrical or conical surface are parabolic points, so the set on a Gaussian sphere cannot have more than two dimensions. It is common to categorize mappings on the Gaussian sphere into zero-, one-, and two-dimensional sets. Zero-dimensional sets consist of coincident points, one-dimensional sets consist of points belonging to curves, and two-dimensional sets occupy a region on the Gaussian sphere. The above three types of sets are also known as clusters in the form of points, curvilinears, and regions, although it should be noted that due to normal estimation errors, the points of point or curvilinear clusters may not coincide exactly or show up as curves.

III. B. 3) K-means clustering of Gaussian mapped points

After unit Gaussian sphere mapping of unit normal vectors of triangles in the neighborhood of each sampled point p_i in the point cloud data, K -means is applied to cluster the Gaussian mapped points. The K -means clustering is one of the most widely used clustering algorithms, and its computational process is very intuitive: in each collection of sampled p_i-Gaussian mapping points, $k^{'}$ elements are selected as the centers of each of the $k^{'}$ clusters (here, in order to be consistent with the above variables (number of neighboring points K and the number of dimensions K)). dimension K) above, the variable $k^{'}$ is chosen as the number of cluster centers). Then the dissimilarity of the remaining elements to the $k^{'}$ cluster centers is calculated separately as:

$$\begin{gathered} d_{ii^{'}} = | x_i - x_{i^{'}} | + | y_i - y_{i^{'}} | + | z_i - z_{i^{'}} | \\ (x_i, y_i, z_i) \in p, (x_i, y_i, z_i) \in p^{k^{'}} \end{gathered} \tag{6}$$

where: $d_{ii^{'}}$ is the Manhattan distance between two points; $i^{'}$ is the set of integers denoting the sequential numbering of the $k^{'}$ clustering centers; and $p^{k'}$ is the $k^{'}$ clustering centers comprising the set. Assign each of these elements to the cluster with the lowest dissimilarity, i.e., the smallest Manhattan distance $d_{ii^{'}}$. Based on the clustering results, the arithmetic mean of the respective dimensions of all elements in the cluster is recalculated as the new center of the $k^{'}$ clusters. All elements in the set are then re-clustered according to the new centers. Repeat the previous step until the clustering results no longer change and output the results.

Among them, the clustering effectiveness indicator for determining the optimal number of clusters is a measure of whether the clustering results produced by the clustering algorithm are optimal, and the indicator takes the number of clusters corresponding to the optimal clustering results as the optimal number of clusters. The existing clustering effectiveness indicators mainly include CH indicator, Wint indicator and Sil indicator. In the course of several comparisons of point cloud data and repetitive experiments, it was concluded that the Sil metric is simple to use and has good evaluation capabilities compared to several other metrics, and the contour coefficient is defined as: 1) Calculate the average distance a_{ii} of the sample ii from the same cluster to the other samples, the smaller its value, the more the sample ii should be clustered to that cluster, so a_{ii} is called the intra-cluster dissimilarity of the sample ii. The a_{ii} mean of all samples in a given cluster is called the cluster dissimilarity of that cluster. 2) Calculate the average distance $b_{iij^{'}}$ of the sample ii to all the other samples of a certain cluster, $j^{'}$ is the other cluster order number, $j^{'} = 1, 2, \cdots, k^{'}$, which is known as the degree of dissimilarity of the sample ii from the other clusters. Defined as the inter-cluster dissimilarity $b_{ii} = \min\{b_{ii1}, b_{ii2}, \cdots, b_{iik'}\}$ of a sample ii, b_{ii} the larger it is, the less sample i belongs to other clusters. 3) Based on the intra-cluster dissimilarity a_i and inter-cluster dissimilarity b_i of sample ii, define the profile coefficient of sample ii as:

$$s_{ii} = \frac{(b_{ii} - a_{ii})}{\max_{(a_{ii}, b_{ii})}} = \begin{cases} 1 - \dfrac{a_{ii}}{b_{ii}} & a_{ii} < b_{ii} \\ 0 & a_{ii} = b_{ii} \\ \dfrac{b_{ii}}{a_{ii}} - 1 & a_{ii} > b_{ii} \end{cases} \tag{7}$$

When s_{ii} is close to 1, it means that sample ii clusters reasonably well. When s_{ii} is close to -1, it means that sample ii should be classified to another cluster more. When s_{ii} is close to 0, it means that the sample ii is on the boundary of two clusters. The average profile coefficient is obtained by finding the profile coefficients of all samples and then averaging them. Its value range is [-1, 1], and the closer the distance of the samples within the clusters, the further the distance of the samples between the clusters, the larger the average contour coefficient, the better the clustering effect. Sil index reflects the intra-cluster closeness and inter-cluster separation of the clustering structure, then, the average contour coefficient of the largest $k^{'}$ is the optimal number of clusters, and the next based on the optimal number of clusters for the judgment of the feature points.

III. B. 4) Judgment of Characteristic Points

Through the above clustering algorithm, the Gaussian mapping points in the neighborhood of the current sampling point P_i are clustered to derive the optimal number of clusters for each target point, and according to the distribution law of Gaussian mapping points of different surfaces mentioned above, it can be seen that: if only one cluster is retained on the unit Gaussian sphere centered on P_i, the potential region of which is a plane, and

Gaussian mapping points have zero-dimensional distribution, it is considered not to be a feature point. If two to four clusters are retained, the potential region is a conic or cylindrical surface or a general tensile surface, and the Gaussian mapping points have a one-dimensional distribution and can be clustered into at most four clusters, the point is considered to be a feature point. If it is a folded edge (two or more faces intersect), the Gaussian mapping points of the sample points on the intersection line will be clustered into two or more clusters on the Gaussian sphere, and then the point is also a feature point. If there are no clusters or greater than four clusters retained on the Gaussian sphere, the point is considered not to be a feature point.

IV. Experimental results and analysis

IV. A. Data sets

In this paper, one publicly available BSDS500 labeled dataset and one tomb mural dataset are selected, which involve different scenes in life, namely indoor scenes, natural landscapes and people, and outdoor landscapes.

BSDS500 is a dataset provided by the Computer Vision Group at the University of Berkeley, which is mainly used for image segmentation and edge detection tasks. The dataset has 200, 100 and 100 images in the training, validation and test sets respectively. The dataset was manually labeled by 5 different people, i.e., each image has 5 labeled maps.

Tomb room mural dataset: the dataset mainly focuses on ancient tomb room mural paintings, and a total of 3000 mural paintings are obtained by cropping the original images to 512×512 size and retaining the clearer and more complete images mainly of figures. The style of these murals is relatively uniform and clear.

IV. B. Evaluation indicators

At present, due to the lack of labeled detailed data sets of tomb chamber frescoes, the evaluation of the obtained line drawings of tomb chamber frescoes still stays on visual perception, i.e., whether the lines of the line drawings are messy and continuous, whether there are too many burrs on the line boundaries or whether the lines of the whole drawing are clear. In order to make a fair comparison, this paper invited 10 professional art faculty members and 50 ordinary people to evaluate the line drawings of the tomb murals obtained by this paper's algorithm and other algorithms, whose main evaluation criteria are 1) whether the lines are correctly segmented or not, and 2) whether they conform to the people's artistic judgment standards. On this occasion, a total of five different types of tomb chamber murals were used for the subjective evaluation.

In order to show the superiority of this paper's algorithm more objectively, three commonly used edge evaluation metrics, ODS, IOS, and AP, are used on the labeled dataset for quantitative evaluation. The general edge detection algorithm obtains an edge detection result that is not a binarized matrix. For subsequent evaluation of the results, it is necessary to transform the obtained edge probability matrix into a binarized result. Generally need to set the threshold η, will be greater than the threshold η set to 0, known as the edge or positive samples, less than the threshold η set to 1, known as non-edge or negative samples.

Precision rate: generally refers to the probability value that the edge pixel obtained is the labeled edge pixel. Recall: generally refers to the probability value that the generated edge pixels account for all labeled edge pixels. The F value: refers to the reconciled average of precision and recall, and β is usually used to adjust the weight of precision and recall:

$$F_{score} = (1+\beta^2)\cdot\frac{Precision\cdot Recall}{\beta^2\cdot Precision+Recall} \tag{8}$$

ODS: Generally known as global optimal, fixed contour threshold, fixed scale of dataset, optimal on the scale of the detection metrics dataset. That is, the same threshold β is set for all images so that the F_{score} value is maximized on the whole dataset.

OIS: Also known as single-image optimal, optimal threshold per image, and image-scale optimal, which means that a different threshold β is chosen for each image to maximize the F_{score} value of that image.

AP: Generally known as average accuracy, this refers to the area under the PR curve.

IV. C. Experimental results

IV. C. 1) Assessment of performance indicators

In order to evaluate the performance of the model on the edge detection task, this paper evaluates the performance metrics on the BSDS500 dataset and the tomb mural dataset. In order to ensure the fairness of the comparison of various algorithms, the edge maps obtained by various algorithms are processed using a non-great suppression algorithm and then compared. In order to visualize the performance of the proposed algorithm, the model is compared with five commonly used algorithms.

The PR curves on different algorithms on the BSDS500 dataset and the tomb mural dataset are shown in

Figures 2 and 3. The proposed algorithm took the state-of-the-art results on both the 2 datasets. In addition, the evaluation results of the two datasets are shown in Table 1, where the algorithm of this paper has achieved some improvement in the 3 common evaluation metrics of edge detection. Among them, on the BSDS500 dataset, the ODS, OIS and AP values of this paper's method are higher than those of the EDTER algorithm by 2.19%, 0.95% and 1.78%, respectively, whereas for the chamber mural dataset, this paper's method improves the ODS, OIS and AP values by 3.35%, 4.05% and 5.24%, respectively, compared with the EDTER algorithm. It shows that the point cloud edge extraction method based on Gaussian mapping clustering in this paper is more effective in extracting the contours of the tomb chamber murals.

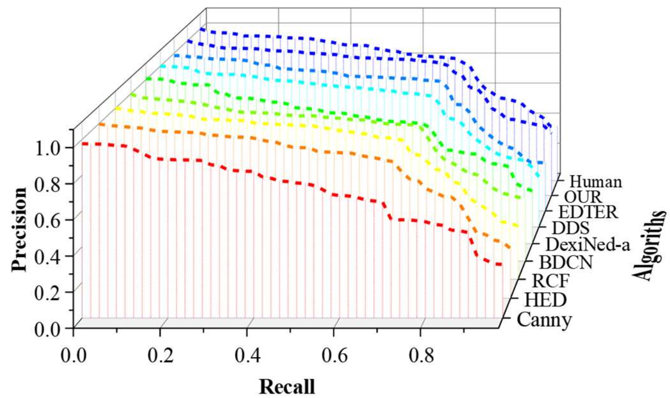

Figure 2: The pr curve of the BSDS500 data set in different algorithms

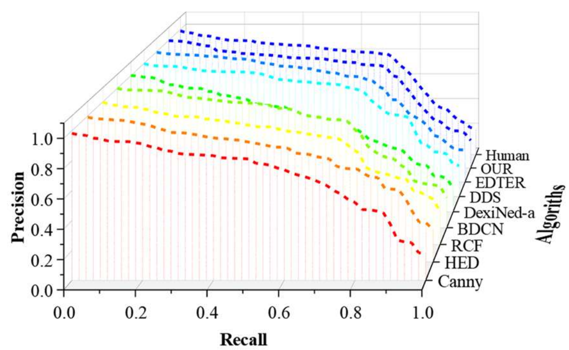

Figure 3: The pr curve of the Tomb murals data set in different algorithms

Table 1: Evaluation results of two data sets

Methods	BSDS500 data set			Tomb murals data set		
	ODS	OIS	AP	ODS	OIS	AP
Canny	0.651	0.679	0.523	0.655	0.673	0.659
HED	0.782	0.805	0.829	0.705	0.738	0.551
RCF	0.813	0.828	0.832	0.74	0.756	0.751
BDCN	0.814	0.837	0.845	0.762	0.789	0.762
DexiNed-a	0.734	0.754	0.688	0.604	0.622	0.505
DDS	0.816	0.832	0.832	0.778	0.792	0.773
EDTER	0.823	0.845	0.844	0.776	0.791	0.801
OUR	0.841	0.853	0.859	0.802	0.823	0.843

IV. C. 2) Edge Extraction Results

In order to verify the effectiveness and robustness of the proposed algorithm, the algorithm of this paper and other algorithms are used to process and compare the same point cloud accordingly. Experiment 1 uses the teapot point cloud as the object point cloud, the number of point clouds is 11200, different algorithms to extract the edge of the teapot point cloud results are compared as shown in Figure 4. The search radius is 35mm, the algorithm of this paper, the extracted edge contour is consistent with the actual contour, the number of extracted edge points is 2520, and the extraction time is 0.65s. The number of extracted edge points of other algorithms is 1018~2027, and the extraction time is 0.69~0.95s. Therefore, the edge points extracted by using this paper's algorithm are more comprehensive, accurate, and fast.

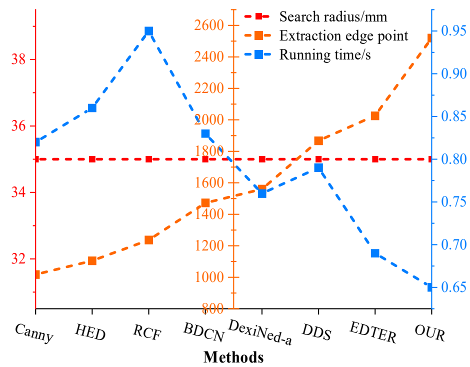

Figure 4: The results of the teapot point cloud edge extracted by different algorithms

Experiment 2 uses a certain chamber mural point cloud as the object point cloud, the number of point clouds is 205,198, and the comparison of the results of different algorithms for extracting the edges of the chamber mural point cloud is shown in Fig. 5. The edge features extracted by the proposed algorithm are richer and more comprehensive, and the running time is less than other algorithms, which greatly improves the efficiency. The number of edge points extracted by this paper's algorithm is 70418, and the extraction time is 1.08 s. While the number of edge points extracted by other algorithms for the sample chamber murals is 45524~62810, and the running time needs 1.13~1.97 s. It can be seen that this paper's Gaussian mapping based clustering point cloud edge extraction algorithm has a better performance of mural feature extraction.

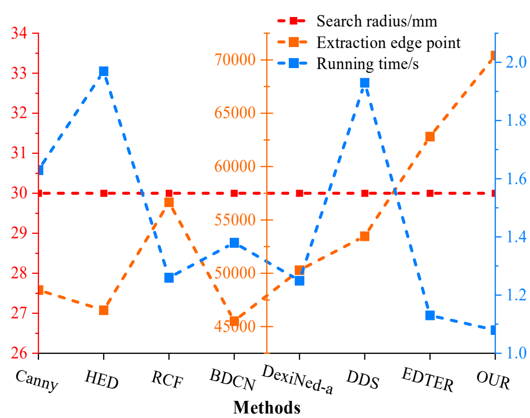

Figure 5: The results of the tomb murals point cloud edge extracted by different algorithms

V. Conclusion

Three-dimensional modeling technology, as a rapidly emerging measurement technology in recent years, has been widely used in many fields. In this paper, the application of 3D modeling technology in cultural genetic conservation is discussed, and the 3D point cloud edge extraction algorithm based on Gaussian mapping clustering is constructed to extract the 3D contour features of the tomb chamber murals as an example, in order to better promote their conservation and dissemination.

The study conducts experiments on the BSDS500 dataset and the homemade tomb chamber mural dataset respectively, and compares them with several algorithms. The results can be obtained that the ODS, OIS and AP values of this paper's algorithms are improved by 2.19%, 0.95% and 1.78% over other algorithms on the BSDS500 dataset, and 3.35%, 4.05% and 5.24% on the tomb chamber mural dataset, respectively. At the same time, the point cloud edge extraction experiments of two groups of objects are carried out, and the number of edge points and running time extracted by this paper's method are better than those of other methods, and the number of edge points and running time extracted for the sample tomb chamber mural are 70418 and 1.08 s. The proposed algorithm has a great improvement in the accuracy and speed of the edge extraction, which confirms the high efficiency of the method.

Based on the application of 3D modeling technology in cultural heritage protection, this paper proposes a 3D point cloud edge extraction algorithm for tomb chamber murals, which achieves very good results on both the public dataset and the tomb chamber mural dataset. In order to better protect and pass on intangible cultural heritage, it is necessary to actively promote the digital transformation of intangible cultural heritage, use high-precision 3D modeling technology to open up communication channels, restore the details of cultural relics and optimize the management mode, so as to make the traditional protection methods combined with digital protection technology, revitalize the use and promote the sustainable development of intangible cultural heritage.

Funding

2024-2025 Henan Province Intangible Cultural Heritage Scientific Research Project "Research on Visualization of Henan Tomb Murals based on the perspective of Inheritance and Protection" Project number: 24HNFY-LX231.

References

[1] Niković, A., Manić, B., Čolić Marković, N., & Krunić, N. (2024). A Contribution to the Integration of International, National and Local Cultural Heritage Protection in Planning Methodology: A Case Study of the Djerdap Area. Land, 13(7), 1026.

[2] Pérez-Gandarillas, L., Manteca, C., Yedra, Á., & Casas, A. (2024). Conservation and protection treatments for cultural heritage: Insights and trends from a bibliometric analysis. Coatings, 14(8), 1027.

[3] Kartono, K., Fadilah, M., Yuliantiningsih, A., & Thakur, A. (2024). Cultural Heritage Protection and Revitalization of Its Local Wisdom: A Case Study. Volksgeist: Jurnal Ilmu Hukum Dan Konstitusi, 245-261.

[4] Gao, Y., Zhang, Q., Wang, X., Huang, Y., Meng, F., & Tao, W. (2024). Multidimensional knowledge discovery of cultural relics resources in the Tang tomb mural category. The Electronic Library, 42(1), 1-22.

[5] Yan, Y., Zhang, R., He, H., Lei, T., Zhang, X., & Jiang, C. (2024). Image Restoration Technology of Tang Dynasty Tomb Murals Using Adversarial Edge Learning. ACM Journal on Computing and Cultural Heritage, 17(3), 1-11.

[6] Shi, J., & Saelee, S. (2025). Goguryeo Tomb Murals in Ji'an: Visual Representation and Educational Practice. International Journal of Education and Literacy Studies, 13(1), 170-178.

[7] Xu, Z., Yang, Y., Fang, Q., Chen, W., Xu, T., Liu, J., & Wang, Z. (2024). A comprehensive dataset for digital restoration of Dunhuang murals. Scientific Data, 11(1), 955.

[8] Yang, J., Cao, J., Yang, H., Li, Y., & Wang, J. (2021). Digitally assisted preservation and restoration of a fragmented mural in a Tang Tomb. Sensing and Imaging, 22, 1-18.

[9] Zheng, Y. (2015). Digital Technology in the protection of cultural heritage Bao Fan Temple mural digital mapping survey. The International Archives of the Photogrammetry, Remote Sensing and Spatial Information Sciences, 40, 495-501.

[10] Papaioannou, K. (2017). The international law on the protection of cultural heritage. IJASOS-International E-Journal of Advances in Social Sciences, 3(7), 257-262.

[11] Bethencourt, M., Fernández-Montblanc, T., Izquierdo, A., González-Duarte, M. M., & Munoz-Mas, C. (2018). Study of the influence of physical, chemical and biological conditions that influence the deterioration and protection of Underwater Cultural Heritage. Science of the Total Environment, 613, 98-114.

[12] Blundo, D. S., Ferrari, A. M., del Hoyo, A. F., Riccardi, M. P., & Muiña, F. E. G. (2018). Improving sustainable cultural heritage restoration work through life cycle assessment based model. Journal of Cultural Heritage, 32, 221-231.

[13] Lebedev, S. V. (2021). Cultural heritage protection in the globalization context. Klironomy Journal, (2), 2.

[14] Gerstenblith, P. (2022). Protecting cultural heritage: The ties between people and places. Cultural heritage and mass atrocities. Getty Publications, Los Angeles, 363-380.

[15] Acampa, G., & Parisi, C. M. (2020). Management of maintenance costs in cultural heritage. In Appraisal and Valuation: Contemporary Issues and New Frontiers (pp. 195-212). Cham: Springer International Publishing.

[16] Revez, M. J., Coghi, P., Rodrigues, J. D., & Vaz Pinto, I. (2021). Analysing the cost-effectiveness of heritage conservation interventions: a methodological proposal within project STORM. International Journal of Architectural Heritage, 15(7), 985-999.

[17] Zheng, S. (2024). Intangible heritage restoration of damaged tomb murals through augmented reality technology: A case study of Zhao Yigong Tomb murals in Tang Dynasty of China. Journal of Cultural Heritage, 69, 135-147.

[18] Liu, Z., & Wang, J. (2024). Protection and Utilization of Historical Sites Using Digital Twins. Buildings, 14(4), 1019.

[19] Li, Z., & Champadaeng, S. (2025). Study of Cultural Heritage and Digital Preservation: The case of Murals of the Northern Yue Temple. International Journal of Education and Literacy Studies, 13(2), 262-268.

[20] Zeng, Z., Qiu, S., Zhang, P., Tang, X., Li, S., Liu, X., & Hu, B. (2024). Virtual restoration of ancient tomb murals based on hyperspectral imaging. Heritage Science, 12(1), 410.

[21] Liu, K., Wu, H., Ji, Y., & Zhu, C. (2022). Archaeology and restoration of costumes in tang tomb murals based on reverse engineering and human-computer interaction technology. Sustainability, 14(10), 6232.

[22] Lin, Y. (2020). Research on interactively digital display for cultural heritage-discovering the Hall of mental cultivation: a digital experience exhibition. Asia-pacific Journal of Convergent Research Interchange, 6(8), 51-67.

[23] Hu, C., Wang, Y., Xia, G., Han, Y., Ma, X., & Jing, G. (2024). The generation method of orthophoto expansion map of arched dome mural based on three-dimensional fine color model. Heritage Science, 12(1).

[24] Guo, M., Fu, Z., Pan, D., Zhou, Y., Huang, M., & Guo, K. (2022). 3D Digital protection and representation of burial ruins based on LiDAR and UAV survey. Measurement and Control, 55(7-8), 555-566.